Flexible 3D shape measurement using projector defocusing: extended measurement range

Song Zhang

Department of Mechanical Engineering, Iowa State University, Ames, Iowa 50011, USA
(song@iastate.edu)

Received December 3, 2009; revised February 5, 2010; accepted February 18, 2010;
posted March 3, 2010 (Doc. ID 120813); published March 19, 2010

A recently proposed flexible 3D shape measurement technique using a defocused projector [Opt. Lett. **34**, 3080 (2009)] shows great potential because of its elimination of projector's gamma calibration. However, it cannot handle step-height surfaces. I present here a technique to extend its measurement range to an arbitrary shape by integrating a binary coding method. A computational framework is also proposed to tackle the problems related to the defocusing. © 2010 Optical Society of America

OCIS codes: 120.0120, 120.2650, 100.5070.

3D shape measurement based on digital sinusoidal fringe-projection techniques has been playing an increasingly important role in optical metrology owing to the rapid advancement of digital video display technology. However, it remains challenging to use an off-the-shelf projector without calibrating its nonlinear gamma.

A recent study showed that by defocusing binary structured patterns, sinusoidal ones can be produced and the problems induced by nonlinear gamma can be eliminated [1]. However, because it only uses one-frequency fringe images, this technique cannot measure step height or discontinuous surfaces. To measure step-height objects, two- [2], multiple- [3], or optimum-wavelength selection [4] techniques have been proposed, essentially to increase the equivalent wavelength to measure an object with large step height. If the longest equivalent wavelength covers the entire range of measurement, arbitrary step height can be measured [5]. There are also techniques that use wavelet-based fringe analysis to step height measurement [6]. However, all these techniques require all fringe patterns to be sinusoidal and thus cannot be applied to this flexible fringe-generation method because, given a degree of defocusing, it is impossible to generate high-quality sinusoidal fringe images for all structured patterns with different stripe widths.

This Letter will introduce a technique that combines binary coding with sinusoidal phase-shifting methods to circumvent this problem. For this method, binary structured patterns are used to generate codewords, that is, to unwrap the phase point by point. Structured patterns are designed so that the codeword is unique for each phase-change period. The projector is properly defocused so that the narrowest binary patterns become sinusoidal ones and the wider ones are deformed to a certain degree. The narrowest binary patterns are spatially phase shifted for phase calculation, and the wider deformed ones are binarized to obtain the codeword. Finally, the codeword is applied to unwrap the phase point by point. Because the projector is not in focus, it causes some problems that will be addressed and handled by a computational framework. Experiments will be presented to verify the performance of the proposed approach.

Phase-shifting methods are widely used in optical metrology because of their speed and accuracy [7]. We use a three-step phase-shifting algorithm with a phase shift of $2\pi/3$, and three fringe images can be written as

$$I_1(x,y) = I'(x,y) + I''(x,y)\cos(\phi - 2\pi/3), \quad (1)$$

$$I_2(x,y) = I'(x,y) + I''(x,y)\cos(\phi), \quad (2)$$

$$I_3(x,y) = I'(x,y) + I''(x,y)\cos(\phi + 2\pi/3), \quad (3)$$

where $I'(x,y)$ is the average intensity, $I''(x,y)$ is the intensity modulation, and $\phi(x,y)$ is the phase to be solved for. Simultaneously solving Eqs. (1)–(3), the phase can be obtained:

$$\phi(x,y) = \tan^{-1}[\sqrt{3}(I_1 - I_3)/(2I_2 - I_1 - I_3)]. \quad (4)$$

This equation provides the wrapped phase with 2π discontinuities. A spatial phase-unwrapping algorithm can be applied to obtain continuous phase [8]. The phase unwrapping is essentially to detect the 2π discontinuities and remove them by adding or subtracting multiple times of 2π point by point. In other words, the phase unwrapping is to find integer number $k(x,y)$ so that

$$\Phi(x,y) = \phi(x,y) + k(x,y) \times 2\pi. \quad (5)$$

Here, $\Phi(x,y)$ denotes the unwrapped phase.

Instead of using a conventional phase-unwrapping algorithm, a binary coding method can be adopted to determine integer $k(x,y)$ [9]. For this method, a sequence of binary images ($I_k^b(x,y)$) are used to obtain the codeword that is designed to be same same as $k(x,y)$. However, unlike the system introduced in [9], the projector is defocused in our system, and some new challenges present and need to be tackled with.

Figure 1 illustrate the schematic diagram for the proposed method. The computer generates a set of binary patterns, with three narrowest ones being shifted spatially. These patterns are sent to a defocused projector. The projector is properly defocused

 © 2010 Optical Society of America

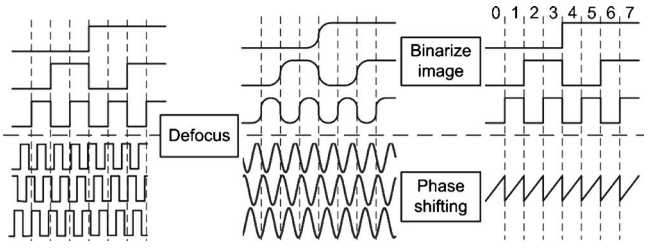

Fig. 1. Schematic diagram of proposed algorithm.

so that the narrowest binary patterns become ideal sinusoidal, while the wider ones are deformed to a certain degree. Three sinusoidal fringe patterns are used to compute the phase using Eq. (4), while the wider ones are binarized to obtain the codeword $k(x,y)$ for phase unwrapping.

Because the object surface might not be uniform, it is necessary to normalize the structured images for codeword generation before binarization. From Eqs. (1)–(3), the maximum and minimum intensity can be obtained pixel by pixel; they are

$$I_{min}(x,y) = I'(x,y) - I''(x,y), \tag{6}$$

$$I_{max}(x,y) = I'(x,y) + I''(x,y). \tag{7}$$

The binary images $I_k^b(x,y)$ can be normalized by equation

$$I_k^{nb}(x,y) = (I_k^b - I_{min})/(I_{max} - I_{min}). \tag{8}$$

This proposed method is tested by a fringe projection system that includes a Dell LED projector (M109S) and The Imaging Source digital USB CCD camera (DMK 21BU04) with a Computar M3514-MP lens F/1.4 with $f=8$ mm. The camera resolution is 640×480. The projector resolution is 858×600, and the projection lens has F/2.0 and $f=16.67$ mm.

We first measure a uniform white flat surface. Figures 2(a) and 2(b) respectively show the widest and narrowest binary images, and Fig. 2(c) shows one of the phase-shifted sinusoidal fringe images. With this set of structured images, the unwrapped phase can be obtained, as shown in Fig. 2(d). However, the phase map clearly shows some problems: undesirable noises. This problem is caused mostly by the defocused projector and the discrete sampling camera. The phase jumps may shift left or right a half pixel owing to the projector defocusing, and the codeword changes may not align with the phase changes, because the camera is a discrete device.

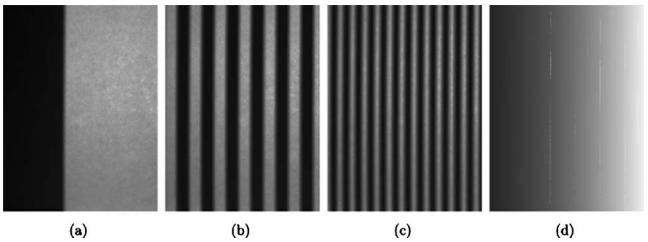

Fig. 2. Experimental results of a flat white surface: (a),(b) widest and narrowest binary patterns; (c) sinusoidal pattern; (d) unwrapped phase map.

Figure 3 shows one cross section of the unwrapped phase map [shown in Fig. 2(d)] and the cross section of the wrapped phase. It indicates that the problematic points occur only to the phase discontinuous neighboring points. To solve this new problem, we developed a computational framework that is divided into three steps: (1) detect and mask incorrect points during binarization stage by referring to the wrapped phase map; (2) identify and mask incorrect binary code points by applying monotonic conditions; and (3) unwrap the masked points applying surface smoothness condition.

Step 1: This step applies to the binarization stage. On the binary image, we identify the binary change points and compute the phase difference between them using the wrapped phase map. If it is less than π, the point is marked as incorrect and will be post processed. Because the codeword is designed to change with the 2π discontinuous places, if the real image does not satisfy this condition, the codeword should be wrong.

Step 2: Because of the design of the digital fringe projection system, the phase map projected by the projector and captured by the camera should be monotonically changing a cross the fringe stripes. Because those incorrect points are sparse points that are close to the phase discontinuous positions, it is feasible to identify them and mark them as incorrect points for further processing by comparing each with its neighboring pixels.

Step 3: For those points require further processing, an additional phase-unwrapping stage is applied. This phase unwrapping applies only locally, from $-N$ to $+N$ points across the fringe stripes. The phase unwrapping is to find integer number k for each masked point (i_0,j_0) to minimize functional

$$\sum_{n=-N}^{n=N} \{\Phi(i_0,j_0+n) - [\phi(i_0,j_0) + k\times 2\pi]\}, \tag{9}$$

assuming the fringe stripe is vertical. The unwrapped phase for (i_0,j_0) point is then $\Phi=\phi+2k\pi$.

Figure 4 shows the results after applying each step for the phase map shown in Fig. 2(d). Figure 4(d) shows one cross section of these phase maps. It should be noted that only a segment of points are displayed and phases are shifted vertically on purpose to better visualize the differences between each step. It clearly shows that the proposed phase-computational framework can successfully remove the induced problems.

To verify the performance of this proposed algorithm, a more complex object sitting in front of a flat

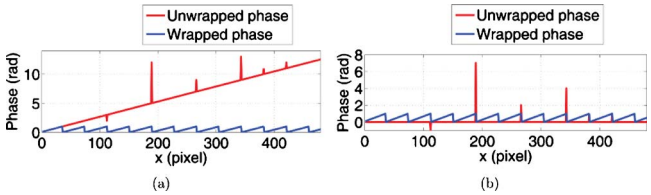

Fig. 3. (Color online) 480th cross section of the wrapped and unwrapped phase. (a) Original unwrapped phase map; (b) map with removed global slope of the unwrapped phase.

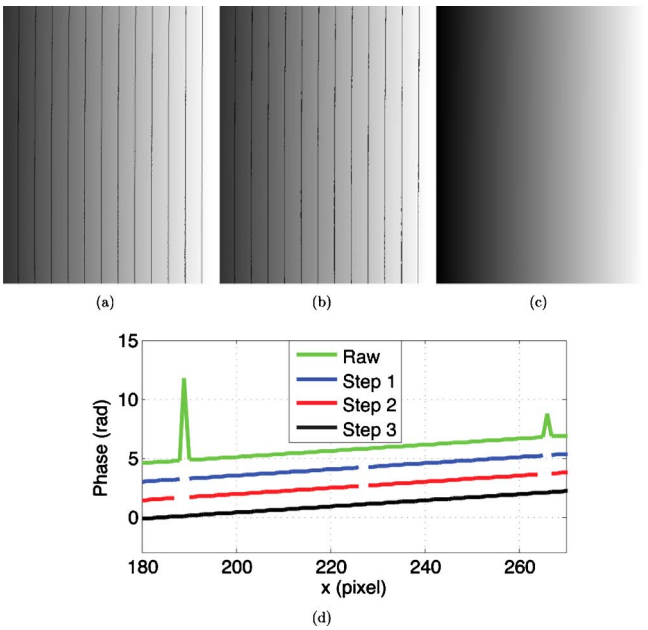

Fig. 4. (Color online) Phase map after applying the computational framework step by step: (a) step 1; (b) step 2; (c) step 3; (d) 480th cross section.

white board is measured. Figure 5 shows the measurement result. Where as Fig. 5(a) shows one of the sinusoidal fringe patterns, Fig. 5(b) shows the measurement result before applying the proposed computational framework. It clearly shows significant errors (spikes in the image). Figure 5(c) shows the result after applying the proposed computation framework. Almost all spikes are gone, and the 3-D shape is correctly recovered. It should be noted that the shadow areas in this example are masked out before any processing. The mask is determined from the fringe quality; for a low-quality fringe point, it is treated as a background. The fringe quality is determined by (1) the intensity of the average image,

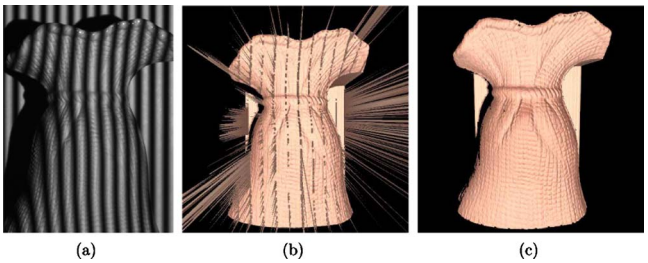

Fig. 5. (Color online) Experimental results of a complex object: (a) one fringe image; (b) 3-D raw data; (c) 3-D data after applying computational framework.

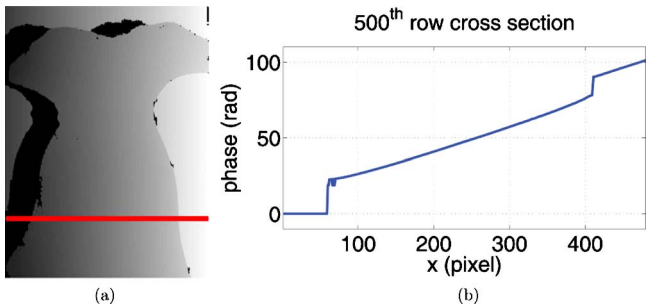

Fig. 6. (Color online) Step-height objects can be correctly measured: (a) unwrapped phase map; (b) cross section.

$I'(x,y)$, and (2) the data modulation $I''(x,y)/I'(x,y)$. A foreground point should have high intensity and should have close to 1 data modulation value.

Because the sculpture and the flat board are separate, this experiment also demonstrated that the proposed approach can measure step height or discontinuous objects. Figure 6(a) shows the unwrapped phase map, and Fig. 6(b) shows one of its cross section (the horizontal line) in the left image; it clearly shows that the phase jumps between some points are far more than 2π. It should be noted that the shadow or the background points are treated as phase value 0.

This Letter has presented a technique to extend the measurement range (i.e., step-height objects and discontinuous surfaces) of the previously proposed flexible 3-D shape measurement technique based on projector defocusing effect. Experiments have verified the feasibility of the proposed approach and the computational framework to handle the phase-unwrapping problems introduced by the projector defocusing.

References

1. S. Lei and S. Zhang, Opt. Lett. **34**, 3080 (2009).
2. C. Polhemus, Appl. Opt. **12**, 2071 (1973).
3. Y.-Y. Cheng and J. C. Wyant, Appl. Opt. **24**, 804 (1985).
4. C. E. Towers, D. P. Towers, and J. D. C. Jones, Opt. Lett. **28**, 887 (2003).
5. S. Zhang, Proc. SPIE **7432**, 74320N (2009).
6. C. Quan, Y. Fu, C. J. Tay, and J. M. Tan, Appl. Opt. **44**, 3284 (2005).
7. D. Malacara, ed., *Optical Shop Testing*, 3rd ed. (Wiley, 2007).
8. D. C. Ghiglia and M. D. Pritt, *Two-Dimensional Phase Unwrapping: Theory, Algorithms, and Software* (Wiley, 1998).
9. G. Sansoni, M. Carocci, and R. Rodella, Appl. Opt. **38**, 6565 (1999).